**Biophysical mechanisms of default mode network function and dysfunction**

*Trang-Anh E. Nghiem*[1], *Vinod Menon*[1-3]

[1]Department of Psychiatry & Behavioral Sciences, Stanford University
[2]Department of Neurology & Neurological Sciences, Stanford University
[3]Wu Tsai Neurosciences Institute, Stanford University

**Address correspondence to:**

Trang-Anh E. Nghiem (tanghiem@stanford.edu), Vinod Menon (menon@stanford.edu)

**Acknowledgements:** This research was supported by the Extramural Research Programs of U.S. NIH: NIMH (R01MH126518) and NINDS (RF1NS086085).

**Author contributions:** T.-A. E. N. and V. M. designed research, T.-A. E. N. performed research, T.-A. E. N. and V. M. analyzed the data and wrote the paper.

**Competing interest:** The authors declare no competing interest.

**Abstract**

The default mode network (DMN) plays a fundamental role in internal cognitive function as well as dysfunction across numerous brain disorders. While human and rodent neuroimaging has revealed DMN suppression by salient external stimuli, the cellular mechanisms orchestrating this process remain unknown. Using whole-brain computational modeling informed by neuronal biophysics and retrograde tracer-derived directional mouse brain connectomics, we demonstrate that stimulation of the insula, involved in salience processing, suppresses DMN activity while within-DMN cingulate stimulation enhances it. Manipulating excitatory-inhibitory balance revealed how localized DMN disruptions propagate to cause distinct patterns of network dysfunction, with both reversals and paradoxical enhancements of normal suppression patterns. Brain-wide response analysis uncovered a functionally segregated frontal network and revealed a hierarchical organization with the DMN distinct from frontal regions. These findings provide a unified framework linking cellular mechanisms to large-scale network dynamics and demonstrate how region-specific disruptions might lead to the patterns of DMN dysfunction observed in brain disorders.

## Introduction

Cognition and its dysfunction in brain disorders emerges from how the brain dynamically regulates activity across distributed networks. One such network, the default mode network (DMN), has emerged as a key player in cognitive function, exhibiting strongly synchronized activity and characteristic suppression to goal relevant external stimuli [1-4]. While extensive research has revealed the DMN's crucial role in internal and self-referential mental processes including mind-wandering, autobiographic memory, and social cognition [1,5,6], the cellular and circuit mechanisms that enable its coordinated activation and suppression remain poorly understood. This mechanistic gap between cellular and network levels of understanding has profound implications for psychiatry and neurology, as it limits our ability to develop targeted interventions for disorders characterized by network dysfunction.

The organizational principles governing DMN function have been extensively documented through human neuroimaging studies. The DMN exhibits strong functional coupling, is suppressed during externally oriented attention, and shows antagonistic relationships with salience and frontoparietal networks involved in salience processing and cognitive control [1]. These properties enable the brain to flexibly switch between internally oriented and externally oriented cognitive states, a fundamental requirement for adaptive behavior. However, despite this rich characterization at the macroscale level, the underlying cellular and circuit mechanisms that enable these dynamic network transitions remain largely unknown.

Altered DMN function, particularly impaired suppression by salient external stimuli, has emerged as a robust biomarker across psychiatric disorders including autism and schizophrenia [7-10]. DMN hyperactivity during tasks requiring external attention has been linked to impaired attention and cognitive flexibility [11-14], social deficits [10], and maladaptive rumination [15] across various conditions. Intriguingly, disorders characterized by altered DMN function show disrupted excitation-inhibition (E/I) balance [16,17], with converging evidence from human neuroimaging [10,18] and animal models [19,20].

The parallel observations of DMN dysfunction and E/I imbalance in the same disorders raise a compelling question: are these phenomena causally linked? If so, how do cellular-level E/I disruptions shape neural circuit function to cause the network-level abnormalities observed in clinical populations? And critically, which specific brain regions are most vulnerable to such E/I disruptions in terms of their impact on global network dynamics? These questions have remained unanswered due to the challenge of bridging scales from neurons to networks, hampering the development of treatment strategies selectively targeting root causes of brain network dysfunction in disorders.

Recent technological advances have begun to address these challenges. Optogenetic manipulation, combined with whole-brain imaging and multi-regional fiber photometry, has enabled researchers to identify a homologue of the human DMN in rodents, anchored in cortical midline structures including retrosplenial cortex (RSC), cingulate cortex (Cg), and prelimbic cortex (PrL) [4,21-23]. These regions show functional connectivity patterns during rest that parallel aspects of the human DMN, providing a valuable model system for investigating cellular mechanisms.

A groundbreaking discovery in this field came from optogenetic studies demonstrating that DMN suppression can be induced by stimulation of the anterior insula, a key hub of the salience/cingulo-opercular network [4]. This finding provides causal evidence for a mechanism that parallels task-related DMN suppression observed in human neuroimaging studies. However, the differential effects of stimulating various nodes within and outside the DMN have not been systematically compared, limiting our understanding of the specific roles of the insula and DMN regions in DMN function. Further, importantly, while these experimental advances establish the insula's causal role in DMN suppression, the cellular and circuit mechanisms underlying this network-level interaction remain unknown.

Here, we address these critical knowledge gaps by developing biophysically informed computational models that bridge cellular mechanisms with large-scale network dynamics. We leverage The Virtual Brain (TVB) simulator [24-28] to implement novel mean-field models of neural dynamics [29]. Our approach integrates the Allen Brain Atlas connectome, which provides experimentally validated, directional connectivity data based on viral tract tracing across 426 regions (Oh, Harris et al. 2014). This comprehensive dataset reveals the precise anatomical organization of circuits linking insula, DMN, and other brain regions, overcoming the directional ambiguity and limitations of crossing-fibers inherent in diffusion imaging (Maier-Hein et al. 2017). By incorporating this high-resolution connectome with biophysically realistic neural dynamics, we create an analytic framework that spans from cellular properties to large-scale network interactions. This multi-scale approach enabled us to systematically investigate how cellular and circuit mechanisms give rise to DMN dynamics while maintaining biological plausibility and revealing principles of network organization.

Our study has four key interconnected objectives. First, we model DMN suppression by insula stimulation to characterize the sufficient signaling properties and circuit mechanisms that can reproduce empirical findings [4]. This analysis is crucial, as computational studies have primarily focused on resting-state dynamics rather than stimulus-evoked responses, leaving open the question of whether whole-brain biophysical models can account for large-scale network responses to specific neuronal perturbations. Second, we investigate how different stimulation targets (insula versus DMN nodes) differentially affect network dynamics [4,22,23]. This comparative approach reveals circuit-specific mechanisms of network control, overcoming limitations of optogenetic studies which were limited to insula stimulation. Third, we examine how region-specific E/I imbalance alters DMN suppression patterns. By systematically reducing inhibitory synaptic strength in different brain regions, we can identify vulnerable nodes and circuit pathways through which cellular disruptions propagate at the network level. Finally, we analyze the larger landscape of brain-wide responses to insula stimulation, particularly regarding potential homologues of the human frontoparietal network. This network, central to cognitive control in humans and implicated in numerous psychiatric disorders [30], has remained elusive in rodent studies due to challenges in capturing task-related activity during whole-brain imaging.

The TVB model incorporates biophysical detail at multiple scales of organization (**Fig. 1**). Each brain region consists of interacting excitatory (E) and inhibitory (I) neural populations whose dynamics are governed by Adaptive Exponential (AdEx) integrate-and-fire equations derived from single-neuron biophysics [29]. These regional nodes are connected according to the empirically determined connectome from the Allen Mouse Brain Atlas, comprising 426 regions

with directional connectivity weights based on viral tract-tracing [31]. This architecture allows us to investigate how cellular properties such as E/I balance shape large-scale network dynamics, with a particular focus on mechanisms enabling DMN function and dysfunction.

Our integrative approach reveals how cellular mechanisms give rise to coordinated network-level phenomena that have previously been observed but not mechanistically explained. The results identify specific circuit pathways mediating DMN suppression and demonstrate how localized disruptions in E/I balance propagate to cause distinct patterns of network dysfunction. Our findings bridge the gap between cellular-level abnormalities implicated in psychiatric disorders and the network-level biomarkers observed in clinical populations. By explaining how different regional E/I disruptions lead to distinct patterns of altered network dynamics, our model may inform more precise diagnostic approaches and guide the development of targeted interventions that address specific circuit abnormalities.

## Results

### *TVB model accounts for DMN suppression upon insula activation*

We investigated whether biophysically realistic neural dynamics coupled with empirical connectomes can reproduce this phenomenon and reveal its underlying mechanisms. We implemented a whole-brain model comprising 426 regional nodes, each containing excitatory (E) and inhibitory (I) neural populations whose dynamics are governed by mean-field integrate-and-fire equations (see Methods). Regions were connected according to the Allen Mouse Brain Atlas connectome derived from viral tract-tracing experiments [31]. To test whether our model could reproduce DMN suppression as observed in optogenetic experiments, we simulated periodic stimulation of the right insula (0.5 seconds every 2 seconds) and analyzed the resulting changes in DMN activity across 100 independent model realizations (**Fig. 2A**).

Our simulations demonstrated significant suppression of key DMN nodes following insula stimulation. Specifically, the ventral retrosplenial cortex (RSCv), ventral cingulate cortex (Cgv), and prelimbic cortex (PrL) all showed reduced activity (Wilcoxon test, $p < 0.001$, FDR corrected; **Fig. 2B**). Interestingly, we observed functional heterogeneity within the cingulate cortex, with dorsal Cg (Cgd) exhibiting enhanced rather than suppressed activity following insula stimulation ($p < 0.001$, FDR corrected). Parameter exploration revealed that DMN suppression emerged robustly when E-to-I connections between regions were sufficiently strong relative to E-to-E connections (ratio between 1.2 and 2.8).

Our model successfully reproduces the empirically observed pattern of DMN suppression following insula stimulation, providing a mechanistic explanation for this phenomenon. The results emphasize that E-to-I connectivity across brain regions is a necessary circuit-level mechanism for DMN suppression, enabling inhibitory neurons to silence local excitatory activity upon receiving inputs from the insula.

### *Stimulation of prefrontal DMN nodes produces effects distinct from insula stimulation*

While insula stimulation suppresses DMN activity, it remains unknown to what extent suppressive effects are specific to the insula. Particularly, how within-DMN stimulation compares to stimulation of the insula, associated with salience circuits and antagonistic to the DMN, remains to be elucidated. Comparing the effects of insula versus within-DMN stimulation can reveal the causal relationship between these networks and clarify the functional roles of different DMN nodes. To address this, we compared the effects of stimulating two putative DMN regions— Cg and PrL—with our established insula stimulation paradigm. This allows us to directly compare the effects of within-DMN to those of insula stimulation on the RSC, believed to be a structural [32] and functional [21,23] hub anchoring the rodent DMN. Using identical stimulation parameters across targets, we analyzed the resulting activity patterns in DMN subregions, focusing on the RSC subdivisions, ventral and dorsal cingulate (Cgv, Cgd), and PrL. We quantified differences in stimulation effects using Wilcoxon tests with FDR correction (**Fig. 3**).

Cingulate stimulation produced strikingly different effects compared to insula stimulation. While insula activation suppressed the RSCv, Cg stimulation significantly enhanced RSCv activity and suppressed the PrL ($p < 0.001$). Conversely, Cg stimulation suppressed agranular and dorsal RSC (RSCagl, RSCd), regions that were less affected by insula stimulation. Effects of stimulating either the Cgv or the Cgd cingulate subdivisions separately yielded similar findings (**Fig. S2A-B**). Effects of Cg stimulation on the RSC were reciprocal, as RSC stimulation (Fig. S2**C-F**) enhanced the Cg overall while also suppressing the PrL ($p < 0.001$). PrL stimulation showed a more complex pattern: like insula stimulation, it suppressed the RSCv, producing effects that were significantly different from those of insula on the RSC ($p > 0.05$). However, unlike insula stimulation, PrL activation failed to suppress the Cgv, indicating a partial dissociation in network effects.

These results reveal a causal antagonism between the DMN and the insula, where cingulate stimulation produces effects opposite to insula stimulation on key DMN nodes. The distinct pattern observed with PrL stimulation suggests this region may serve as an interface between networks, sharing characteristics with both DMN and salience circuits.

***Regional E/I balance controls DMN suppression patterns***

E/I imbalance has been implicated in various psychiatric disorders, including autism [16,17], which also show altered DMN function. However, the causal relationship between cellular E/I balance and network-level DMN function remains unknown. To address this, we systematically investigated how localized E/I imbalance affects DMN suppression by selectively reducing inhibitory synaptic conductance in different DMN regions. We manipulated I synaptic conductance (from baseline 5 nS to 4 nS) controlling I synaptic strength and hence E/I balance in RSC, Cg, and PrL separately, while measuring the resulting changes in network dynamics during insula stimulation (**Fig. 3**). Statistical comparisons were performed using Wilcoxon tests with FDR correction.

Each regional E/I disruption produced a distinct pattern of altered DMN suppression. E/I imbalance in the RSC caused a complete loss of insula-mediated suppression in RSC subregions, effectively reversing the normal response pattern, while paradoxically increasing suppression in

Cgv and PrL (**Fig. 3A-B**). E/I disruption in Cg led to loss of Cgv suppression, attenuated RSCv suppression, and enhanced PrL suppression (**Fig. 3C-D**). When E/I imbalance was introduced in the PrL, suppression was abolished specifically in this region while RSC and Cg responses remained largely intact (**Fig. 3E-F**). These region-specific patterns were maintained across different levels of E/I imbalance: consistent findings were found at a less severe E/I imbalance, arising from I conductance of 4.5 nS (**Fig. S2**). This result underscores the robustness of our findings to the value of this biophysical parameter.

These results reveal that sufficient inhibitory conductance is necessary for normal DMN suppression, and that the network-wide consequences of E/I disruption depend critically on which region is affected.

***TVB modeling reveals a putative mouse homolog of a frontal network***

The frontoparietal network plays a critical role in cognitive control and working memory in humans and is activated during salient stimulus processing. However, whether a homologous network exists in rodents remains unclear. We analyzed brain-wide responses to insula stimulation, focusing on regions beyond the established DMN and insula. We examined activity changes in frontal regions including the orbitofrontal cortex (ORB), frontal pole (FRP), and infralimbic cortex (ILA), as well as the posterior parietal cortex (PTLp), which might constitute a putative mouse frontoparietal network (**Fig. 4A-B**).

Insula stimulation produced robust activation in specific frontal regions, with lateral (ORBl) and medial (ORBm) orbitofrontal cortex, frontal pole, and caudoputamen all showing significant increases in firing rates ($p < 0.001$, FDR corrected). This activation pattern showed regional specificity; ventrolateral orbitofrontal cortex (ORBvl) and posterior parietal cortex were suppressed rather than enhanced (**Fig. 4B**).

Next, characterized the intrinsic network organization of these regions in relation to DMN and the insula (**Fig. 5C-D**). Functional connectivity analysis revealed that orbitofrontal regions showed strong coupling with insula subdivisions, while the PTLp was more strongly correlated with the RSC. Hierarchical clustering identified two distinct network clusters: a DMN-like cluster containing RSC, Cgd, and PTLp, and a frontal cluster containing ORB, FRP, PrL, ILA grouped with the AI (**Fig. 5D**).

These findings provide evidence for a mouse homolog of the human frontal network, though without a lateral posterior parietal component.

## Discussion

Our computational investigation reveals fundamental mechanisms linking cellular-level processes to large-scale brain network dynamics. Using biophysically informed whole-brain modeling, we demonstrate how specific cellular and circuit properties give rise to coordinated DMN function and its modulation by the insula. Our analysis yields several key insights that bridge microscale and macroscale brain organization, function, and dysfunction in disorders.

First, we show that DMN suppression by insula stimulation requires specific excitatory-inhibitory circuit interactions, particularly a balanced ratio of E-to-I versus E-to-E connectivity between regions. Results characterize necessary mechanisms for phenomena previously observed with rodent optogenetics and only through correlations in human neuroimaging. Second, we demonstrate that insula stimulation produces coordinated modulation of the DMN that differs fundamentally from Cg and PrL stimulation, with antagonistic effects on key nodes like the RSC. This dissociation provides mechanistic evidence for the insula's specialized role in network control and explains the functional basis of the well-documented task-off versus task-on network dichotomy. Third, we show how localized disruptions in E/I balance [16,17] propagate to cause distinct patterns of network dysfunction, with RSC emerging as a particularly vulnerable node whose disruption can both reverse and paradoxically enhance normal suppression patterns. This finding links cellular-level mechanisms to system-wide alterations and provides a framework for understanding heterogeneous manifestations of psychiatric disorders [7]. Fourth, we uncovered evidence for a segregated frontal network, anchored in the orbitofrontal cortex and frontal pole, that displays opposing responses to the DMN following insula stimulation. The integration of cellular biophysics with large-scale network dynamics represents a significant advance in bridging traditionally separate domains of neuroscience investigation [29], and provides a unified framework for understanding both normal brain function and its disruption in brain disorders.

***Cellular mechanisms underlying insula-mediated DMN suppression***

We modeled DMN suppression by insula stimulation to identify signaling properties and circuit mechanisms that can reproduce empirical findings (Menon, Cerri et al. 2023). Our biophysically informed model successfully reproduces empirically observed DMN suppression by insula stimulation, providing mechanistic insights into this fundamental network interaction. Specifically, we found that insula stimulation leads to suppression of key DMN nodes, including the ventral retrosplenial cortex (RSCv), ventral cingulate cortex (Cgv), and prelimbic cortex (PrL), consistent with experimental observations in rodents [4,22,23]. This suppression emerges from the interplay between excitatory and inhibitory processes across regions, revealing for the first time how cellular-level mechanisms enable the salience network to modulate DMN activity.

Our analysis also revealed that E-to-I connectivity across regions is a crucial mechanism enabling DMN suppression. We found that DMN suppression only emerges when E-to-I connections between regions are sufficiently strong relative to E-to-E connections, specifically when this ratio falls between 1.2 and 2.8. While human neuroimaging studies have established correlational relationships between insula and DMN activity [3], and optogenetic studies have demonstrated causality (Menon, Cerri et al. 2023), our model provides the first mechanistic demonstration how this interaction can occur at a cellular level.

Our results reveal important regional dissociations within the DMN. The selective suppression of RSCv is particularly noteworthy given its direct connections with the hippocampus [31], a key DMN node associated with spatial navigation in rodents [23,33] and both spatial navigation and memory in humans [1]. Moreover, we observed a striking dissociation within the cingulate cortex – while Cgv shows suppression aligned with other DMN regions, Cgd exhibits enhanced activity similar to the insula. This finding helps resolve an apparent paradox in the field where the dorsal anterior cingulate cortex in humans shows stronger functional coupling with the salience network

than the DMN [2,34]. Our model thus provides a mechanistic explanation for the functional heterogeneity observed in both cingulate and retrosplenial cortices.

Importantly, our simulations demonstrate that insula activation can result in coordinated DMN suppression, providing a mechanistic basis for decades of human neuroimaging observations showing DMN deactivation during attention to external stimuli [2,35]. The model generates specific predictions about the temporal dynamics of suppression across DMN nodes that can be tested in future experimental work.

***Differential effects of insula versus DMN node stimulation***

Next, we investigated how different stimulation targets (insula versus putative DMN nodes) differentially affect network dynamics. This comparative approach revealed circuit-specific mechanisms of network control, overcoming limitations of optogenetic studies which were limited to insula stimulation. We found that insula stimulation produces coordinated DMN suppression that differs fundamentally from stimulation of cingulate and prelimbic regions, providing mechanistic evidence for the insula's specialized role in network control. While insula stimulation led to suppression of both RSCv and Cgv, stimulating other putative DMN nodes produces markedly different effects. Specifically, stimulation of both Cg subdivisions, together or separately, showed opposite effects to insula stimulation, enhancing rather than suppressing neural activity in all three RSC subdivisions. These anatomical dissociations align with recent evidence showing distinct connectivity patterns and functional roles of dorsal versus ventral cingulate regions in rodents (Oh et al. 2014) and humans (Vogt et al. 2019).

In contrast, PrL stimulation partly mimics insula effects on RSC, with no significant differences between PrL and insula stimulation on RSC activity. Like the insula, PrL stimulation enhanced Cgd activation, but unlike the insula, failed to suppress Cgv. This intermediate pattern suggests that the PrL's functional properties may prove a bridge between DMN and the insula. This functional position is supported by the PrL's unique anatomical organization, as it receives direct inputs from the insula unlike other DMN regions (Oh et al. 2014). Hierarchical clustering analyses of GCaMP recordings further support this organization, showing RSC and Cg are closely aligned while PrL is more distant, with insula being most distant (Chao et al. 2023). These findings reveal a dynamic organization where the PrL may serve as a connector hub between networks.

These results demonstrate a causal antagonism between the DMN and “task-positive” networks, where Cg stimulation produces effects opposite to insula stimulation on key DMN nodes. This functional organization helps explain how the brain maintains separation between internally-oriented and externally-oriented attentional states, while allowing for controlled transitions between them. The opposite effects of Cg and insula stimulation provide a mechanistic basis for the antagonistic relationship observed between these networks during cognitive tasks and has implications for understanding disorders characterized by altered network switching.

The differential responses to regional stimulation have important implications for understanding network control principles. The fact that insula stimulation drives coordinated suppression across specific DMN nodes, while stimulation of DMN nodes produces variable effects, suggests the

insula serves as a master control node for modulating DMN states. This aligns with its proposed role in salience detection and network switching (Sridharan et al. 2008, Menon and Uddin 2010). The PrL's ability to partially replicate insula effects while maintaining unique influence over Cg suggests it might serve as a local control point for fine-tuning network interactions.

***E/I balance in network function and dysfunction***

Our systematic investigation of excitatory-inhibitory balance reveals its fundamental role in maintaining normal DMN function and providing a mechanistic link between cellular disruptions and network-level abnormalities. By reducing inhibitory conductance in specific DMN nodes while measuring responses to insula stimulation, we identified regional vulnerabilities and circuit pathways through which cellular disruptions propagate to cause network dysfunction. Understanding how E/I imbalance affects this suppression mechanism is particularly relevant for disorders characterized by altered sensory processing and attention switching [16,20,36-38].

Our examination of E/I balance revealed its fundamental role in maintaining normal DMN function. When I synaptic conductance was reduced in specific DMN nodes, we observed distinct patterns of altered DMN suppression associated with insula stimulation. Reduction of inhibitory conductance in the RSC led to a complete reversal of the normal suppression pattern. Instead of the typical suppression seen with insula stimulation, both dorsal and agranular RSC showed enhanced activity, while paradoxically increasing suppression in the ventral cingulate cortex (Cgv) and prelimbic cortex (PrL) (**Figure 4**). Together with the necessity of stronger inter-regional E-to-I compared to E-to-I connections, the need for sufficient I conductance to observe DMN suppression suggest that insula stimulation preferentially activates inhibitory interneurons in DMN regions, which then suppress local excitatory activity. The results hence reveal that appropriate E/I balance is crucial for maintaining normal network activity in response to insula stimulation.

Importantly, each region's E/I disruption produced a distinct pattern of network alterations (**Figure 4**). Most strikingly, E/I imbalance in the RSC had the most widespread effects, altering responses across RSC subdivisions as well as Cg and PrL dynamics evoked by stimulation. The localized effects of PrL E/I disruption, compared to the more distributed alterations seen with RSC and Cg manipulation, suggests a functional organization where certain regions exert more control over network dynamics.

These region-specific patterns of altered network function have particular relevance for neuropsychiatric disorders. The heterogeneous E/I-imbalance-induced changes we observed parallel the complex patterns of altered connectivity documented in conditions like autism, where both hyper- and hypo-connectivity have been reported in different subdivisions of posterior cingulate and retrosplenial cortex [39]. Our model suggests such mixed connectivity patterns may arise from localized E/I disruptions in specific network nodes rather than requiring multiple distinct pathologies.

Our findings provide a mechanistic framework for understanding how cellular abnormalities manifest as specific patterns of network dysfunction. E/I imbalance appears to fundamentally alter how the DMN responds to salient stimuli, potentially explaining attention and sensory

processing abnormalities observed across various disorders. The fact that different regional E/I disruptions produce distinct patterns of network dysfunction may help explain the heterogeneity of symptoms seen clinically, even within diagnostic categories. Moreover, these results suggest that therapeutic approaches might need to be tailored to address region-specific E/I abnormalities, as the same intervention might have different effects depending on which brain region is primarily affected.

***Distinct functional segregation of the DMN from frontal networks in the mouse brain***

Understanding the organization of large-scale brain networks in rodents is fundamental for translational neuroscience, yet substantial questions remain about homology to human networks. While recent studies have advanced our understanding of the DMN and salience network in rodents [21], [4,40,41], a clear rodent homolog of the human frontoparietal network has remained elusive. This gap exists partly due to methodological challenges in recording whole-brain activity during cognitive tasks in rodents and partly due to fundamental anatomical differences—rodents lack a clear homolog to the human dorsolateral prefrontal cortex, a key node of the human frontoparietal network. Our insula stimulation approach provides a novel method to probe network interactions, addressing how the DMN functionally relates to other association networks in the mouse brain.

To investigate these relationships, we systematically examined insula-evoked responses in multiple frontal and parietal association regions. This expanded analysis included orbitofrontal cortex (ORB), frontal pole (FRP), infralimbic areas (ILA), and posterior parietal cortex (PTLp) - regions that might constitute putative homologs of components of the human frontoparietal system. We specifically targeted higher-order association regions while excluding primary and secondary motor and somatosensory cortices to focus on regions involved in cognitive rather than sensorimotor processing. This approach allowed us to map the functional relationships between the DMN and frontal association areas during both task-evoked (insula stimulation) and intrinsic (resting-state) conditions, revealing network organization principles that have not been previously characterized in the mouse brain.

Our analysis of brain-wide responses to insula stimulation and resting-state functional connectivity reveals a hierarchical organization with the DMN as a distinct functional entity (**Fig. 5D**). The first cluster comprises DMN regions including dorsal and ventral retrosplenial cortex (RSCd, RSCv), agranular retrosplenial cortex (RSCagl), dorsal cingulate cortex (Cgd), and posterior parietal cortex (PTLp). This tight grouping confirms the coherent nature of the rodent DMN as a functional unit and demonstrates its segregation from other brain areas.

The second functional cluster contains the AI, prelimbic cortex (PrL), infralimbic areas (ILA), ventral cingulate cortex (Cgv), frontal pole (FRP), and orbitofrontal regions (ORBm, ORBl, ORBvl). The functional properties of these regions suggest they form a coherent network involved in executive control, decision-making, and salience processing - functions analogous to those performed by the frontoparietal and salience networks in humans. Each component within this network contributes distinct yet complementary functions: the frontal pole (FRP) plays a critical role in higher-order cognitive operations [42,43]; the prelimbic cortex (PrL) mediates executive control and goal-directed decision-making processes; the infralimbic cortex (ILA) and

ventral cingulate cortex (Cgv) regulate emotional responses and autonomic functions; and the orbitofrontal regions (ORB) specialize in value-based computations and reward processing. Together, these regions form an integrated functional system that enables adaptive behavioral responses to changing environmental demands - a system that operates distinctly from, and often in opposition to, the internally-focused processing of the DMN.

Notably, the mouse posterior parietal cortex (PTLp) aligns functionally with the DMN rather than with frontal regions, as demonstrated by both its response to insula stimulation and its intrinsic connectivity patterns. This organization bears intriguing parallels to the human angular gyrus, which is incorporated within the DMN, distinct from the intraparietal sulcus and supramarginal gyrus that form part of the human frontoparietal network [44]. The rodent posterior parietal cortex is considerably less expanded than in primates and lacks clear homologs to these specialized parietal subregions. Our findings suggest a fundamental principle of DMN organization in rodents: the DMN incorporates posterior parietal functions that, through evolutionary expansion in primates, have become distributed across multiple specialized networks.

Critically, our simulations suggest that the DMN in mice displays unique response properties to insula stimulation compared to frontal regions. While insula stimulation suppresses activity in DMN nodes, it enhances activity in frontal regions, highlighting the antagonistic relationship between these networks. The separation from the DMN is particularly significant as it demonstrates that these frontal regions operate as functionally distinct networks with different activation patterns and connectivity profiles.

These findings have significant implications for understanding DMN function and dysfunction in neuropsychiatric disorders. The clear functional dissociation between the DMN and frontal networks provides a framework for investigating how cellular-level disruptions propagate differently through these distinct networks. This network organization and its neurophysiological underpinnings establish a foundation for more precise translational models of DMN dysfunction in conditions such as autism and schizophrenia, where disrupted communication between DMN and frontal networks impairs cognitive flexibility and social processing. By identifying specific cellular properties governing these network interactions, our work enables targeted investigation of how molecular and circuit alterations differentially impact DMN versus frontal-executive systems in disease states. Though fundamental mechanisms of network interaction appear conserved across species, their implementation through specific neural circuits differs substantially, necessitating careful consideration when translating findings between rodent models and human clinical applications.

**Conclusions**

Our study provides a unified understanding of the cellular-scale mechanisms orchestrating DMN dynamics, bridging basic and systems neuroscience. Through biophysically detailed models incorporating tracer-derived directed connectomes, we reveal how DMN suppression emerges from circuit interactions and demonstrate the specific role of anterior insula in regulating distinct DMN nodes. Our work also uncovers a distinct frontal network in the mouse brain, functionally

segregated from the DMN and showing opposing responses to insula stimulation—a fundamental organization principle previously uncharacterized in rodent literature.

Critically, our findings demonstrate that sufficient excitatory-inhibitory balance is necessary for normal DMN function, as localized disruptions in E/I balance lead to widespread alterations in network dynamics. The functional dissociation between the DMN and frontal networks provides a framework for investigating how cellular-level disruptions propagate differently through these distinct networks. This establishes a foundation for more precise translational models of DMN dysfunction in conditions such as autism and schizophrenia, where disrupted communication between the DMN and frontal networks impairs cognitive flexibility and social processing.

Our modeling approach links specific patterns of network dysfunction to localized E/I disruptions, informing more precise diagnostic approaches and targeted interventions. While fundamental mechanisms of network interaction appear conserved across species, their implementation through specific neural circuits differs substantially, requiring careful consideration when translating between rodent models and human clinical applications. These insights into causal links between cellular mechanisms and large-scale brain dynamics advance both our basic understanding of brain organization and clinical approaches to treating network-level dysfunction in neuropsychiatric disorders.

## Methods

### *Biophysical neural network model*

To model the biophysical mechanisms underlying whole-brain dynamics and DMN function, we developed a biophysical model of adaptive exponential (AdEx) neurons of whole-brain dynamics in the mouse brain. The model was implemented in The Virtual Brain (TVB) simulator [24,25] based our previous implementation for the human brain [29]. Each region comprises an E and an I neural populations whose firing rate dynamics reproduce the behavior of AdEx spiking neuron networks (Gerstner and Brette 2009). In these spiking network models, the neural membrane voltage $V$ for a neuron of type $\mu \in \{E, I\}$ is described by

$$C_m \frac{dV}{dt} = g_L \left(E_{L_\mu} - V\right) + g_L \, \Delta_\mu e_\mu^{\,V - V_{thr}/\Delta_\mu} + I_{syn},$$

with $C_m = 200\ pF$ is the membrane capacity, $g_L = 10\ nS$ the leakage conductance, $E_{L_\mu} = -63\ mV, -65\ mV$ for $\mu = E, I$ the cell-type-dependent leakage reversal potential, $\Delta_\mu = 2\ mV, 0.5\ mV$ and $\Delta_I = 0.5\ mV$ the cell-type-dependent sodium sharpness, $V_{thr} = -50\ mV$ the spiking threshold, and $I_{syn}$ the voltage-dependent input synaptic current of the neuron, that varies according to

$$I_{syn} = \sum_\mu G_\mu \left(E_\mu - V\right).$$

$G_\mu$ is the time-dependent synaptic conductance modelled by the exponential function

$$G_\mu(t) = Q_\mu \sum_{k \in pre_\mu} \Theta\left(t - t_k^{sp}\right) e^{-\left(t - t_k^{sp}\right)/u}$$

Which decays at a rate controlled by time constant $u = 5\ ms$, and is incremented by a cell-type-dependent constant $Q_\mu = 1.5\ nS, 5\ nS$ across all brain regions for $\mu = E, I$ at each time $t_k^{sp}$ a spike is produced by neuron $k$. The sum is computed over all presynaptic neurons of type $\mu$, and $\Theta(\cdot)$ is the Heaviside function (1 when its argument is positive and 0 otherwise). Note that the adaptive part of the AdEx model is not in use here as adaptation can be considered near zero during awake, high-neuromodulation states.

***Mean-field model***

To bridge biophysical single-neuron dynamics to population firing rates at the brain region level without the prohibitive computational cost of simulating one equation for each of the many neurons within any region, we use a mean-field model of AdEx neural networks. Here, the mean-field model captures the firing rate of a mean neuron of any given type in a neural network as a response to the firing rates of other mean neurons of its own type and of all other types within the network. In the master equation formalism (), this means that the firing rate $r_\mu$ of the mean neuron of type $\mu$ in an AdEx network is given by

$$T\frac{dr_\mu}{dt} = F_\mu - r_\mu$$

Where $x_\mu$ is the vector of firing rates for population $\mu \in \{E, I\}$ for each simulated network node and $T$ is a time constant. The transfer function $F_\mu(\cdot)$, which relates each population's output rate to the input it receives from itself and other populations is a cell-type-dependent polynomial whose parameters were fitted to reproduce the input-output relations of integrate-and-fire neurons in spiking simulations [45].

***Inter-regional coupling in TVB***

To couple multiple regional mean field models together, we can write the previous differential equation as follows:

$$T\frac{dr_{\mu_i}}{dt} = F_{\mu_i}(r_\mu^{ext} + r_{\mu_i} + r_{\nu_i,\ \nu\neq\mu}) - r_{\mu_i}$$

For a mean neuron of type $\mu$ in region $i$, with $\nu$ is the other cell type than $\mu$ and $r_\mu^{ext}$ the external input from other brain regions i.e.

$$r_\mu^{ext}(t) = \sum_{j\neq i} C_{j\to i}\, R_\mu r_{E\,j}\left(t - \frac{D_{ij}}{v_{ax}}\right) + r_{noise}$$

Where E neurons project synaptically onto both E and I neurons in other regions, with the ratio between $R_E = 1$ and varying $R_I$ controlling relative projection strengths to E and to I neurons across regions. The directed, weighted graph of inter-regional synaptic connections $C_{j\to i}$ was taken from a 426-region tracer-derived structural connectome from the Allen Mouse Brain Institute [31]. Inter-regional synaptic delays were modelled based on the matrix of tract lengths $D_{ij}$

from the same data [31], with axonal propagation speed $v_{ax} = 3m/s$. Synaptic weights and delays were set as equal from both brain hemispheres.

***DMN emergence analysis***

All simulations whose analyses are shown in figures from this point on are with a ratio between E-to-E and E-to-I inter-regional coupling strengths of $R = 1.4$.

***Insula, Cg, and PrL stimulation***

Our primary analysis focuses on the insula to account for experimental findings reporting DMN suppression as observed with fMRI in response to optogenetic stimulation of the right anterior insula. We focus our stimulation on the agranular insular cortex rather than the granular insular cortex due to its stronger connectivity with limbic, autonomic, and higher-order cognitive regions (REF). Unlike granular insular cortex, which primarily processes sensory inputs, AI is more integrative, playing a critical role in emotion, decision-making, and interoception (REFs). Evidence suggests that the mouse AI can play a major role in modulating neural dynamics across brain networks, as it serves as a structural outflow hub as opposed to the RSC node of the DMN which constitutes an inflow hub of the mouse structural connectome (Coletta). Targeting AI allows us to better understand its contribution to brain network dynamics and neural processing and link to prior optogenetic stimulation studies.

For comparison, we consider the Cg and PrL as control stimulation sites. This allows us to compare salience circuit stimulation with within-DMN stimulation on the DMN and particularly its RSC node. As evidence for the RSC's role as a structural [32] and functional [21,23] hub anchoring the rodent DMN has been provided by prior literature, it is crucial to understand causal influences of within-DMN as compared to salience circuit modulations on RSC dynamics.

To study the impact of stimulation on DMN dynamics, stimuli were square-wave pulses of firing rate of amplitude 0.1 Hz delivered for 0.5 s every 2 s for 150 s to match optogenetic protocols (REF) after an initial transient of 5 s to all three subdivisions of the right agranular insula. The same procedure was repeated with the right Cg subdivisions together (Fig. 3) and separately (Fig. S2) and the right PrL stimulated instead of the insula. This procedure was repeated 100 times with different random seeds yield distinct initial conditions as well as random noise realizations.

The resulting simulated time series were averaged separately for each seed over stimulus presentations, i.e. over 2s long windows in which each stimulus was presented after 1s. For plotting, the trial-averaged evoked response was further downsampled to 10 Hz and averaged separately over all subdivisions of the RSC, all subdivisions of the Cg, and all subdivisions of the PrL.

### *Local loss of I synaptic conductance*

To study the impact of regional loss of I synaptic conductance, we modified the $Q_I$ parameter in all subregions of the RSC bilaterally, then separately in all subregions of the Cg bilaterally, then separately in the PrL bilaterally. For each altered region, $Q_I$ took the values 4 nS and 4.5 nS. In all other, unchanged regions, $Q_I$ was maintained to the value of 5 nS. For each altered region and value of local $Q_I$, 100 simulations were run with different random seeds. In each simulation, the insula was stimulated as described before. Analyses and statistics were performed in the same way as for previous sections.

### *Statistical testing*

To evaluate the significance of suppression and enhancement in response to stimulation, we considered the difference between the trial-averaged, time-averaged evoked activity in the second before and in that after the stimulus in each trial. This difference was computed in each of the 100 independent random realizations of the model. Statistical testing compared this difference across independent realizations to zero with a two-tailed one-sample Wilcoxon test.

To compare two sets of stimulation responses, either for two different stimulation targets or for two different levels of inhibitory conductance, simulations were conducted with the same 100 random seeds across both sets of simulations. For each random seed, a pair of simulations with the same initial conditions and noise realization, differing only in the condition of interest i.e. stimulation site or inhibitory conductance, was obtained. This allowed us to compute differences between post- and pre-stimulus activity as before and perform a paired Wilcoxon signed-rank test. FDR correction for multiple comparisons was applied over the tests on signals from all RSC, Cg, and PrL subdivision considered.

### *Code availability*

All simulation codes will be made publicly available upon publication.

## References


1 Menon, V. 20 years of the default mode network: A review and synthesis. *Neuron* **111**, 2469-2487 (2023).

2 Seeley, W. W. *et al.* Dissociable intrinsic connectivity networks for salience processing and executive control. *Journal of neuroscience* **27**, 2349-2356 (2007).

3 Sridharan, D., Levitin, D. J. & Menon, V. A critical role for the right fronto-insular cortex in switching between central-executive and default-mode networks. *Proceedings of the National Academy of Sciences* **105**, 12569-12574 (2008).

4 Menon, V. *et al.* Optogenetic stimulation of anterior insular cortex neurons in male rats reveals causal mechanisms underlying suppression of the default mode network by the salience network. *Nature Communications* **14**, 866 (2023).

5 Greicius, M. D., Krasnow, B., Reiss, A. L. & Menon, V. Functional connectivity in the resting brain: a network analysis of the default mode hypothesis. *Proceedings of the National Academy of Sciences* **100**, 253-258 (2003).

6 Molnar-Szakacs, I. & Uddin, L. Q. Self-processing and the default mode network: interactions with the mirror neuron system. *Frontiers in human neuroscience* **7**, 571 (2013).

7 Menon, V. Large-scale brain networks and psychopathology: a unifying triple network model. *Trends in cognitive sciences* **15**, 483-506 (2011).

8 Goodkind, M. *et al.* Identification of a common neurobiological substrate for mental illness. *JAMA psychiatry* **72**, 305-315 (2015).

9 McTeague, L. M. *et al.* Identification of common neural circuit disruptions in cognitive control across psychiatric disorders. *American Journal of Psychiatry* **174**, 676-685 (2017).

10 Padmanabhan, A., Lynch, C. J., Schaer, M. & Menon, V. The default mode network in autism. *Biological Psychiatry: Cognitive Neuroscience and Neuroimaging* **2**, 476-486 (2017).

11 Weissman, D. H., Roberts, K., Visscher, K. & Woldorff, M. The neural bases of momentary lapses in attention. *Nature neuroscience* **9**, 971-978 (2006).

12 Menon, V., Anagnoson, R., Mathalon, D., Glover, G. & Pfefferbaum, A. Functional neuroanatomy of auditory working memory in schizophrenia: relation to positive and negative symptoms. *Neuroimage* **13**, 433-446 (2001).

13 Kwon, H., Reiss, A. L. & Menon, V. Neural basis of protracted developmental changes in visuo-spatial working memory. *Proceedings of the National Academy of Sciences* **99**, 13336-13341 (2002).

14 Garrity, A. G. *et al.* Aberrant "default mode" functional connectivity in schizophrenia. *American journal of psychiatry* **164**, 450-457 (2007).

15 Zhou, H.-X. *et al.* Rumination and the default mode network: Meta-analysis of brain imaging studies and implications for depression. *Neuroimage* **206**, 116287 (2020).

16 Rubenstein, J. L. R. & Merzenich, M. M. Model of autism: increased ratio of excitation/inhibition in key neural systems. *Genes Brain and Behavior* **2**, 255-267, doi:10.1034/j.1601-183X.2003.00037.x (2003).

17 Nelson, S. B. & Valakh, V. Excitatory/inhibitory balance and circuit homeostasis in autism spectrum disorders. *Neuron* **87**, 684-698 (2015).

18 Supekar, K., Ryali, S., Mistry, P. & Menon, V. Aberrant dynamics of cognitive control and motor circuits predict distinct restricted and repetitive behaviors in children with autism. *Nature Communications* **12**, 3537 (2021).

19 Yizhar, O. *et al.* Neocortical excitation/inhibition balance in information processing and social dysfunction. *Nature* **477**, 171-178 (2011).
20 Antoine, M. W., Langberg, T., Schnepel, P. & Feldman, D. E. Increased Excitation-Inhibition Ratio Stabilizes Synapse and Circuit Excitability in Four Autism Mouse Models. *Neuron* **101**, 648-+, doi:10.1016/j.neuron.2018.12.026 (2019).
21 Gutierrez-Barragan, D. *et al.* Unique spatiotemporal fMRI dynamics in the awake mouse brain. *Current biology* **32**, 631-644. e636 (2022).
22 Chao, T.-H. H. *et al.* Neuronal dynamics of the default mode network and anterior insular cortex: Intrinsic properties and modulation by salient stimuli. *Science Advances* **9**, eade5732 (2023).
23 Nghiem, T.-A. E. *et al.* Space wandering in the rodent default mode network. *Proceedings of the National Academy of Sciences* **121**, e2315167121 (2024).
24 Sanz Leon, P. *et al.* The Virtual Brain: a simulator of primate brain network dynamics. *Frontiers in neuroinformatics* **7**, 10 (2013).
25 Sanz-Leon, P., Knock, S. A., Spiegler, A. & Jirsa, V. K. Mathematical framework for large-scale brain network modeling in The Virtual Brain. *Neuroimage* **111**, 385-430 (2015).
26 Schirner, M., McIntosh, A. R., Jirsa, V., Deco, G. & Ritter, P. Inferring multi-scale neural mechanisms with brain network modelling. *elife* **7**, e28927 (2018).
27 Zimmermann, J. *et al.* Differentiation of Alzheimer's disease based on local and global parameters in personalized Virtual Brain models. *NeuroImage: Clinical* **19**, 240-251 (2018).
28 Kringelbach, M. L., Perl, Y. S., Tagliazucchi, E. & Deco, G. Toward naturalistic neuroscience: Mechanisms underlying the flattening of brain hierarchy in movie-watching compared to rest and task. *Science Advances* **9**, eade6049 (2023).
29 Goldman, J. S. *et al.* A comprehensive neural simulation of slow-wave sleep and highly responsive wakefulness dynamics. *bioRxiv* (2021).
30 Menon, V. & D'Esposito, M. The role of PFC networks in cognitive control and executive function. *Neuropsychopharmacology* **47**, 90-103 (2022).
31 Oh, S. W. *et al.* A mesoscale connectome of the mouse brain. *Nature* **508**, 207-214 (2014).
32 Coletta, L. *et al.* Network structure of the mouse brain connectome with voxel resolution. *Science advances* **6**, eabb7187 (2020).
33 Alexander, A. S., Place, R., Starrett, M. J., Chrastil, E. R. & Nitz, D. A. Rethinking retrosplenial cortex: perspectives and predictions. *Neuron* **111**, 150-175 (2023).
34 Menon, V. & Uddin, L. Q. Saliency, switching, attention and control: a network model of insula function. *Brain structure and function* **214**, 655-667 (2010).
35 Fox, M. D. *et al.* The human brain is intrinsically organized into dynamic, anticorrelated functional networks. *Proceedings of the National Academy of Sciences* **102**, 9673-9678 (2005).
36 Calvin, O. L. & Redish, A. D. Global disruption in excitation-inhibition balance can cause localized network dysfunction and Schizophrenia-like context-integration deficits. *Plos Computational Biology* **17**, doi:ARTN e1008985

10.1371/journal.pcbi.1008985 (2021).
37 Foss-Feig, J. H. *et al.* Searching for Cross-Diagnostic Convergence: Neural Mechanisms Governing Excitation and Inhibition Balance in Schizophrenia and Autism Spectrum Disorders. *Biological Psychiatry* **81**, 848-861, doi:10.1016/j.biopsych.2017.03.005 (2017).

38 Gao, R. & Penzes, P. Common Mechanisms of Excitatory and Inhibitory Imbalance in Schizophrenia and Autism Spectrum Disorders. *Current Molecular Medicine* **15**, 146-167, doi:Doi 10.2174/1566524015666150303003028 (2015).
39 Lynch, C. J. *et al.* Default mode network in childhood autism: posteromedial cortex heterogeneity and relationship with social deficits. *Biological psychiatry* **74**, 212-219 (2013).
40 Gozzi, A. & Schwarz, A. J. Large-scale functional connectivity networks in the rodent brain. *Neuroimage* **127**, 496-509 (2016).
41 Tsai, P.-J. *et al.* Converging structural and functional evidence for a rat salience network. *Biological psychiatry* **88**, 867-878 (2020).
42 Tsujimoto, S., Genovesio, A. & Wise, S. P. Frontal pole cortex: encoding ends at the end of the endbrain. *Trends in cognitive sciences* **15**, 169-176 (2011).
43 Bludau, S. *et al.* Cytoarchitecture, probability maps and functions of the human frontal pole. *Neuroimage* **93**, 260-275 (2014).
44 Uddin, L. Q. *et al.* Dissociable connectivity within human angular gyrus and intraparietal sulcus: evidence from functional and structural connectivity. *Cerebral cortex* **20**, 2636-2646 (2010).
45 Di Volo, M., Romagnoni, A., Capone, C. & Destexhe, A. Biologically realistic mean-field models of conductance-based networks of spiking neurons with adaptation. *Neural computation* **31**, 653-680 (2019).

## Figures

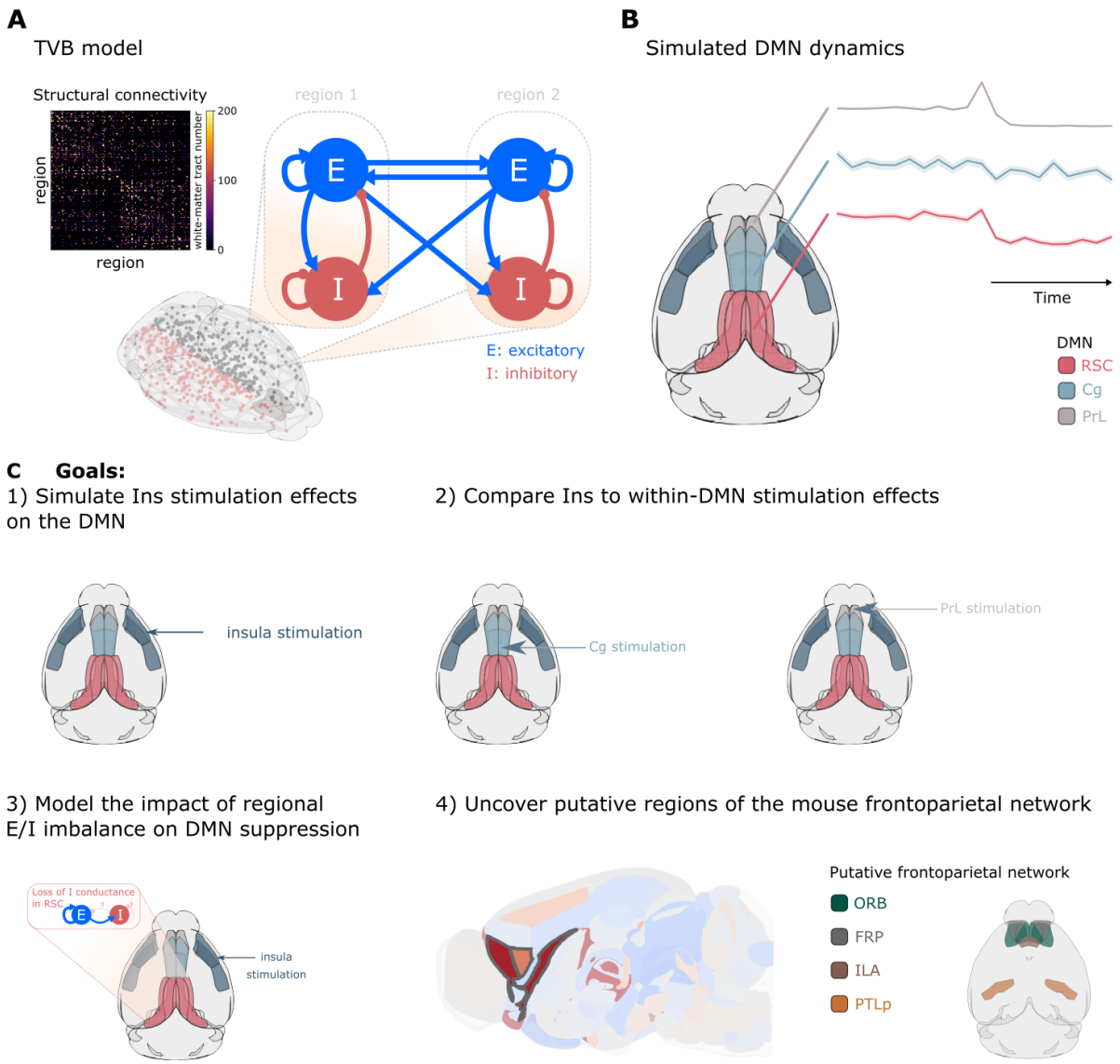


**Figure 1. Model architecture and study goals. (A)** Diagram showing The Virtual Brain model architecture incorporating excitatory (E) and inhibitory (I) neural populations and their interactions. **(B)** Left: Anatomical regions of interest showing DMN nodes (RSC, Cg, PrL). Right: Example of simulated population dynamics. **(C)** Schematic overview of study aims.

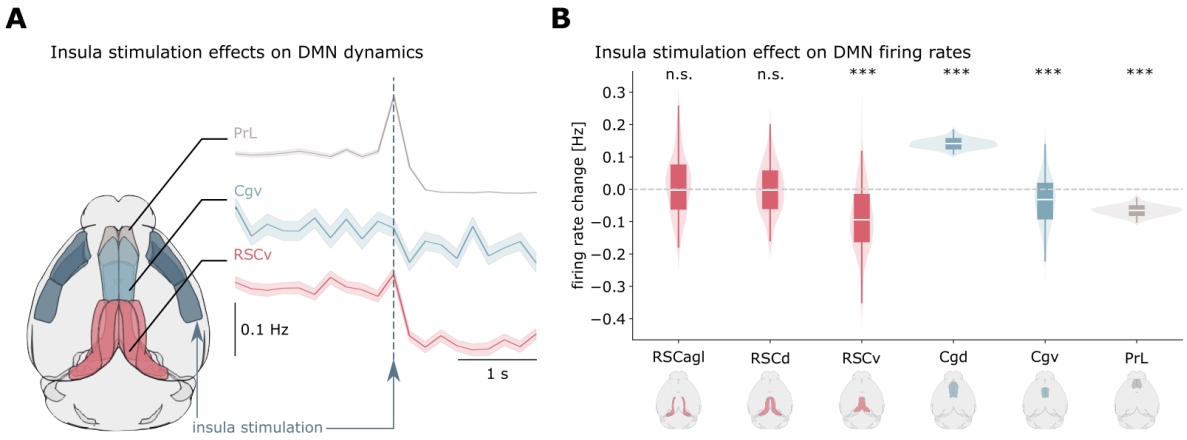


**Figure 2. Insula stimulation produces coordinated DMN suppression. (A)** Schematic showing insula stimulation and resulting DMN node dynamics. Time courses show suppression of ventral RSC, ventral Cg, and PrL following insula stimulation. **(B)** Violin plots quantifying firing rate changes across DMN subregions, demonstrating selective suppression of specific DMN nodes. Results show coordinated suppression of ventral RSC, ventral Cg (Cgv), and PrL, with enhanced activation of dorsal Cg (Cgd), revealing functional heterogeneity within the network. The findings demonstrate that our model can account for empirically observed DMN suppression by insula activation. Violin plots quantify firing rate changes in DMN subregions under each condition, averaged over 100 model realizations.

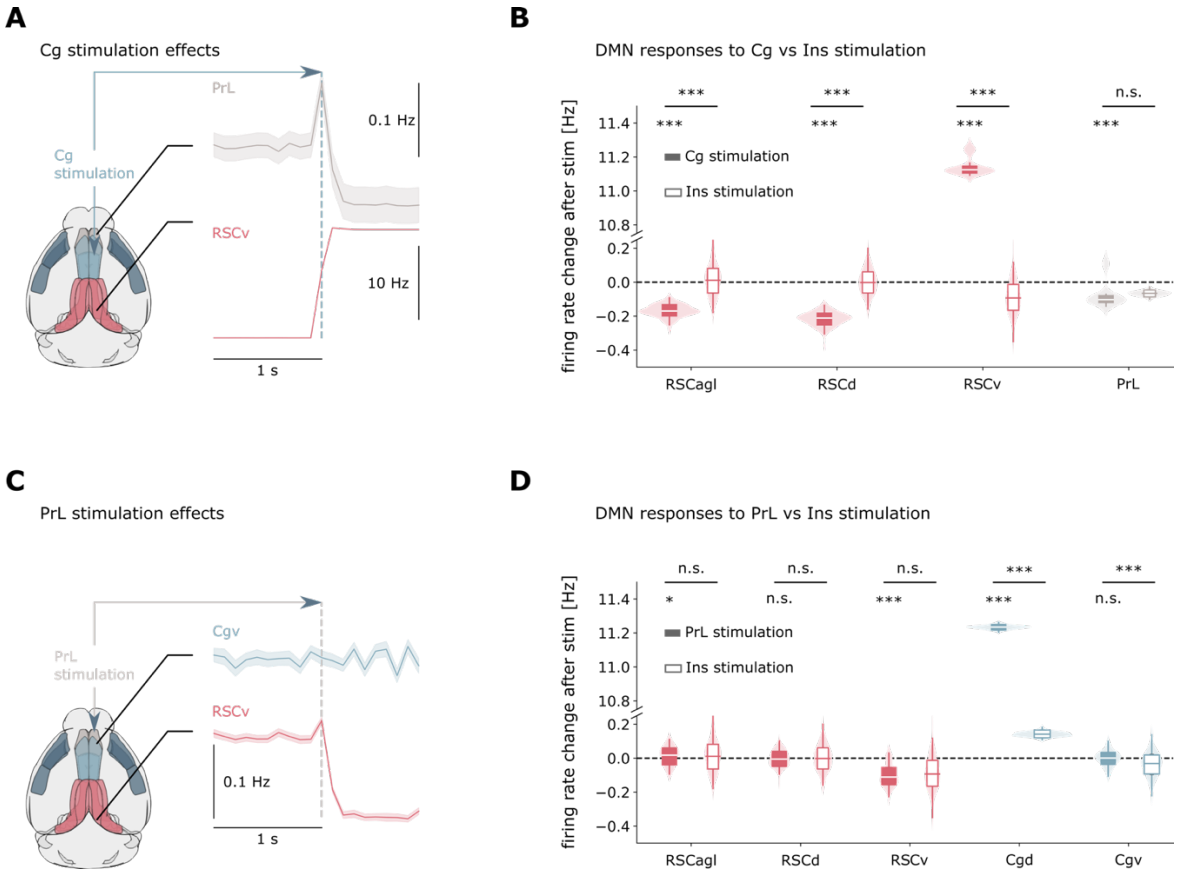


**Figure 3. Distinct network effects of DMN node stimulation. (A-B)** Stimulation of Cg produces opposite effects to insula stimulation on RSC, demonstrating network antagonism between DMN and salience network circuits. **(C-D)** PrL stimulation partially mimics insula effects on RSC but shows distinct impact on Cg, suggesting PrL may serve as interface between networks. Results reveal hierarchical organization of network control mechanisms.

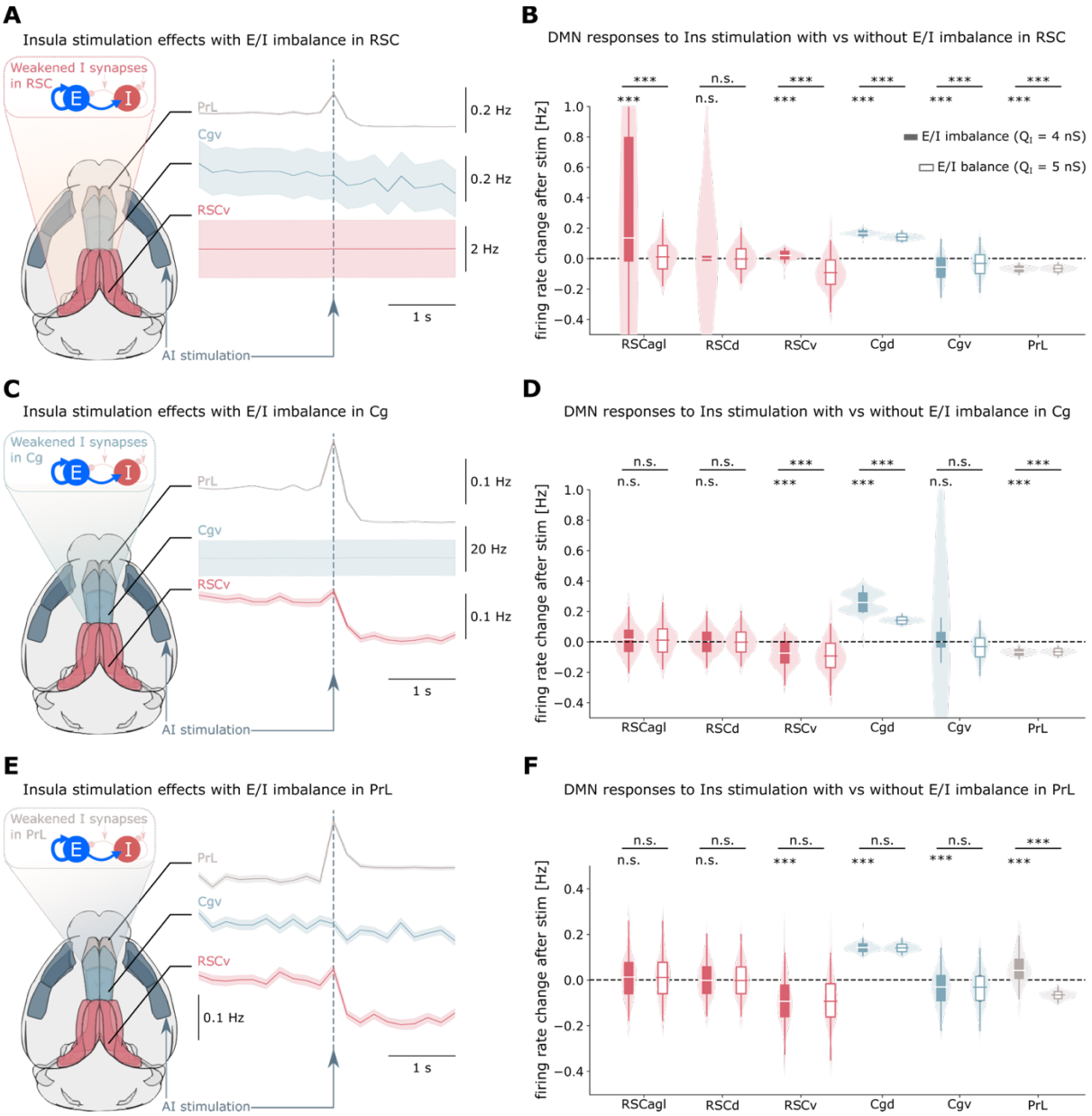


**Figure 4. Effects of regional E/I balance due to weakened I synapses on DMN suppression patterns. (A-B)** E/I imbalance in the RSC leads to reversal of normal suppression pattern - both dorsal and ventral RSC show enhanced activity rather than suppression following insula stimulation, while paradoxically increasing suppression in ventral Cg and PrL. **(C-D)** E/I imbalance in the Cg results in loss of ventral Cg suppression, attenuated RSCv suppression, and enhanced PrL suppression, suggesting multiple pathways mediate DMN suppression. **(E-F)** E/I imbalance in the PrL enhanced PrL activity but did not affect suppression in the RSC or Cg, consistent with the PrL's relative disengagement from the DMN and potential dual involvement to both the DMN and salience circuits. Results demonstrate how localized cellular disruption can lead to widespread network alterations.

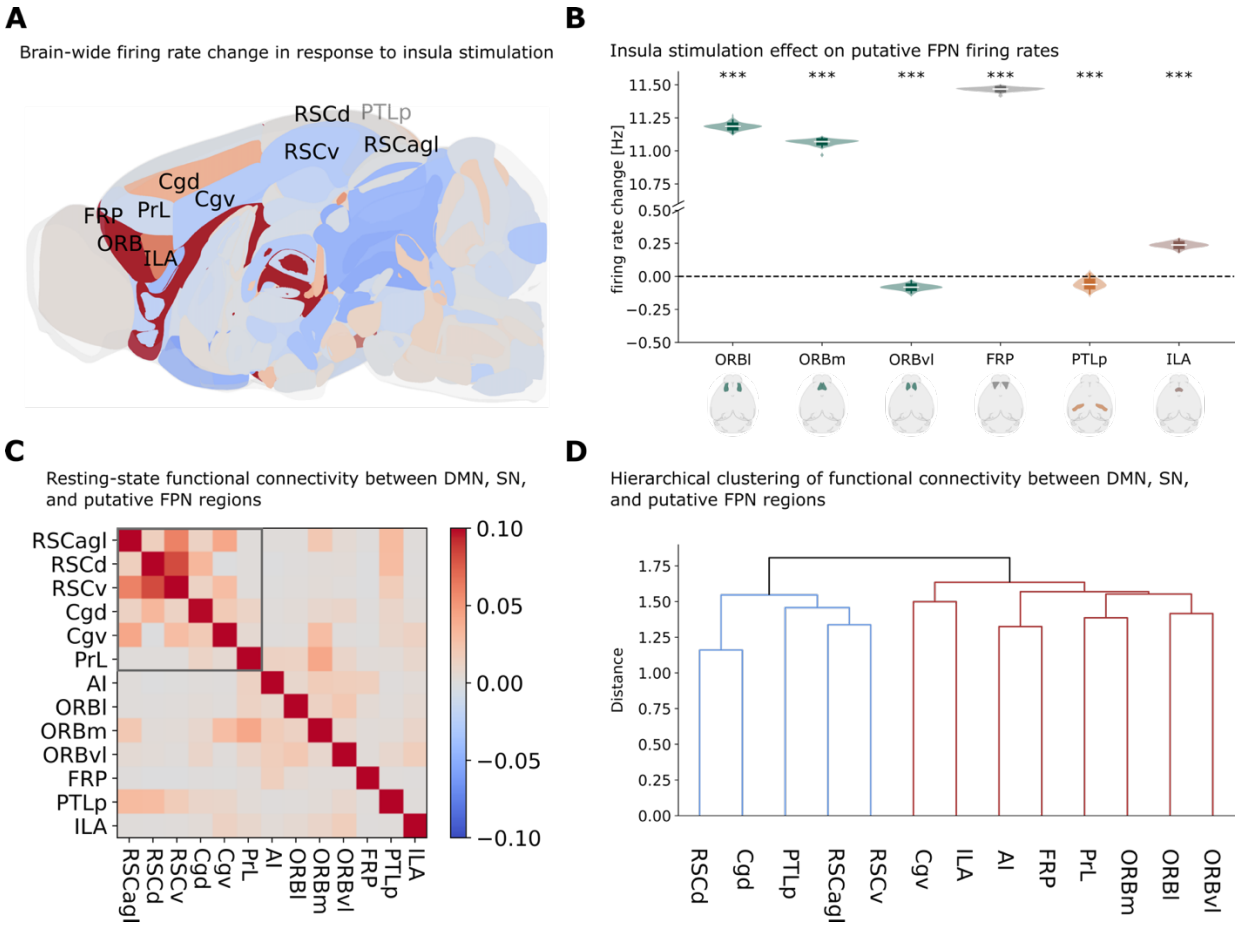


**Figure 5. Identification and characterization of a putative rodent CEN. (A)** Sagittal view of simulated right-hemisphere firing rate responses to right insula stimulation. Color indicates changes in firing rate between after and before insula stimulation, with red indicating enhancement and blue denoting suppression. Visible (black) and hidden (gray) regions of the DMN, SN, and putative CEN are labeled. **(B)** Violin plots quantifying firing rate changes across putative CEN subregions, demonstrating selective suppression of specific CEN nodes including the ORBl, ORBm, FRP, and CP. **(C-D)** Resting-state functional connectivity matrix (**C**) and hierarchical clustering dendrogram (**D**) among right DMN, SN, and putative CEN subdivisions. A spontaneous cluster emerges between DMN regions (**D**, red), encompassing the PTLp but not the PrL that appears more aligned with the SN and CEN during resting state but with the DMN upon insula stimulation.

## Supplementary Materials

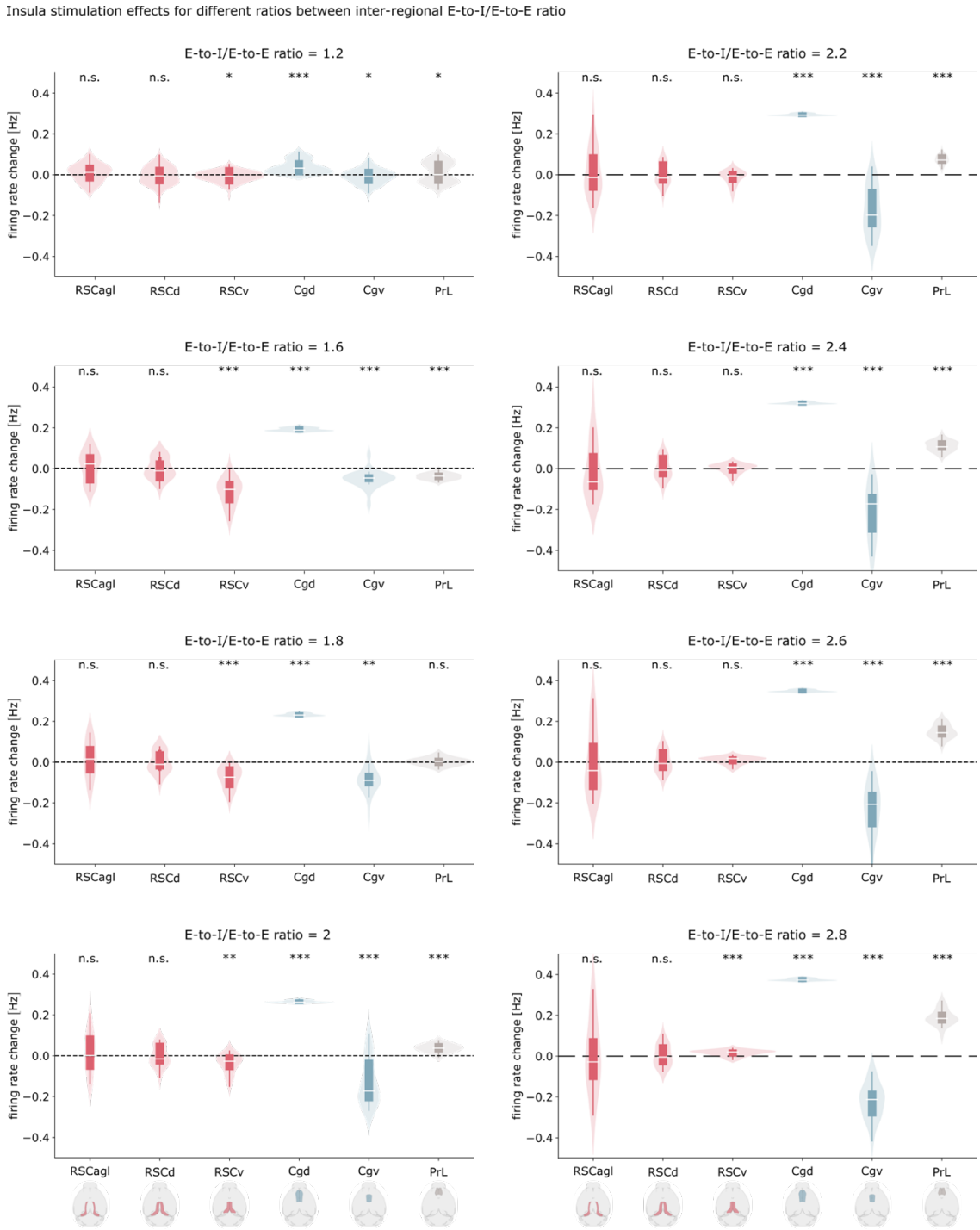


**Figure S1. Insula stimulation produces coordinated DMN suppression across a range of ratios between E-to-E and E-to-I inter-regional projection weights.** The RSC is found to be suppressed RSCv across ratios from 1.2 to 2.2, the Cgv across ratios from 1.2 to 2.8, and the PrL

across ratios from 1.2 to 1.8. The results show that DMN suppression is robustly obtained ratios provided stronger E-to-I than E-to-E weights.

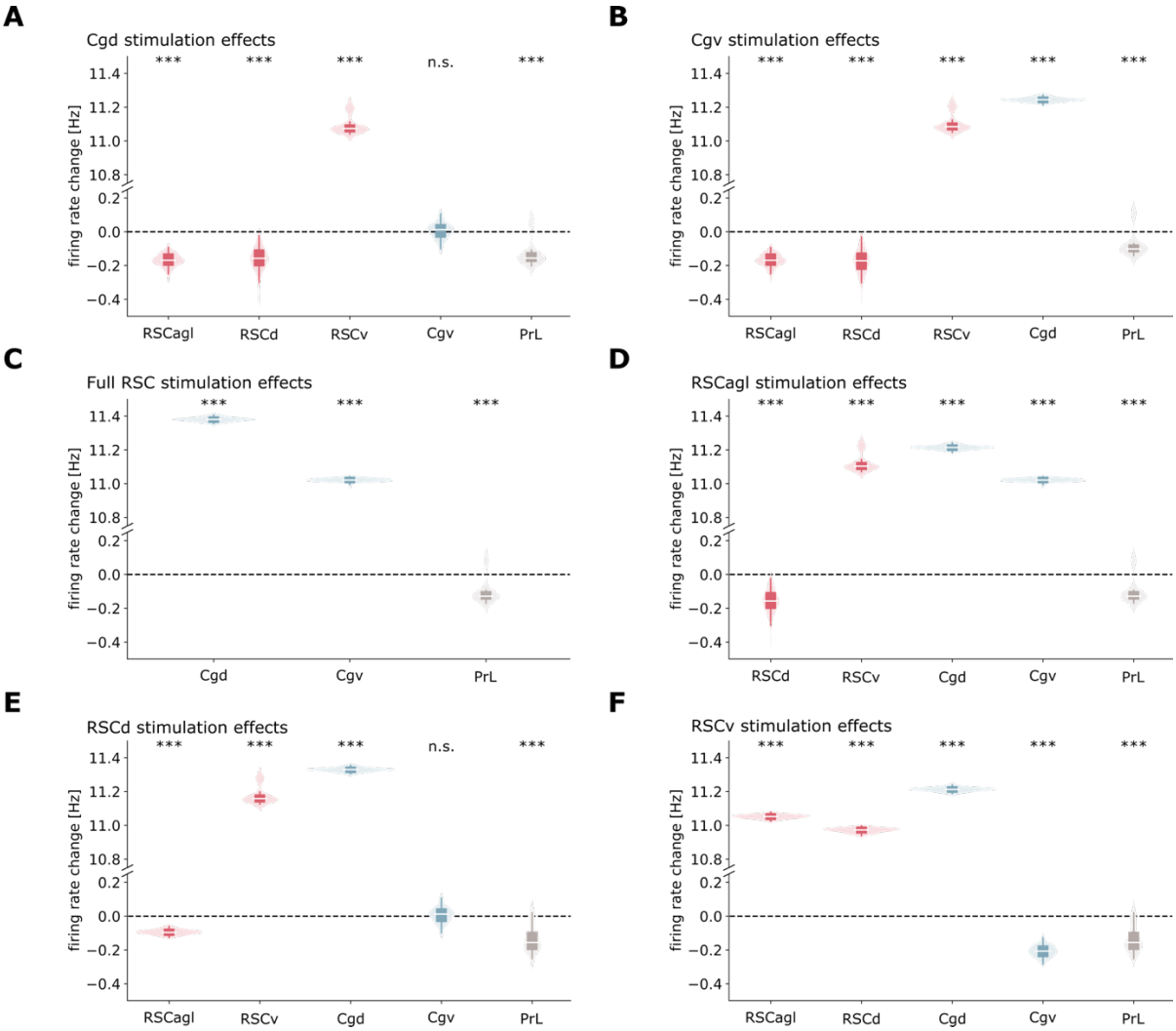


**Figure S2. Effects of RSC and Cg subdivision stimulation on DMN activity. (A-B)** Stimulation of the Cgd **(A)** and Cgd **(B)** both enhance RSCv dynamics while suppressing other RSC subdivisions as well as the PrL. **(C-F)** Stimulation of the full RSC **(C)** as well as of its RSCagl **(D)**, RSCd **(E)**, and RSCv **(F)** subdivisions separately all enhance the Cgd and suppress the PrL. Effects on the Cgv are subdivision-specific, with net enhancement from full RSC stimulation. The results show the Cg and RSC, when stimulated, mutually enhance each other, unlike the insula when stimulated (Figure 2).

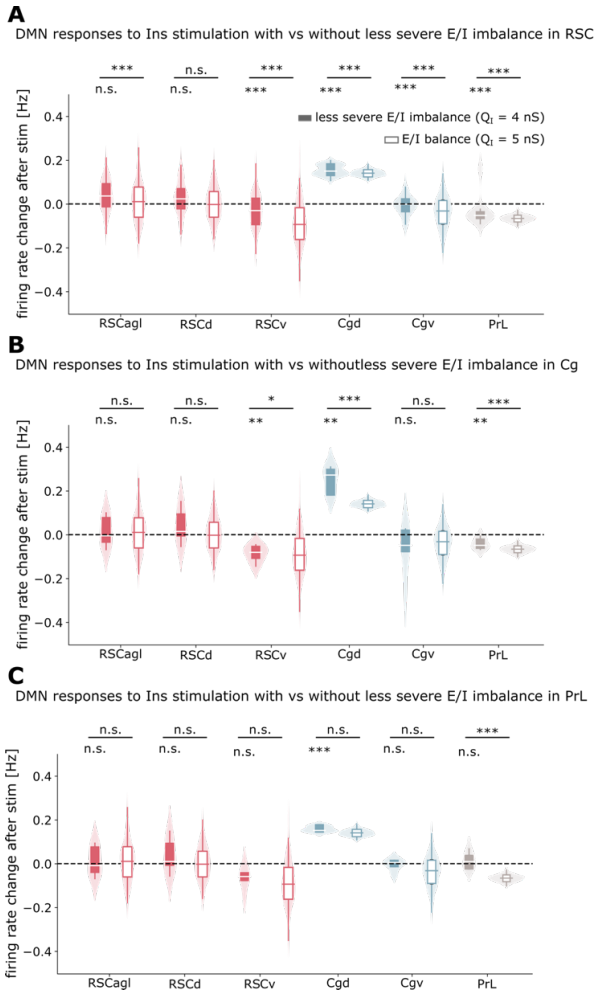


**Figure S3. Robust effects of regional E/I imbalance on DMN suppression patterns across imbalance severity levels.** Less severe E/I imbalance resulting from less weakened I synapses ($Q_I$ = 4.5 nS) is used in simulations here compared to Figure 4. **(A)** E/I imbalance in RSC leads to reversal of normal suppression pattern - both dorsal and ventral RSC show enhanced activity rather than suppression following insula stimulation, while paradoxically increasing suppression in ventral Cg and PrL. **(B)** E/I imbalance in Cg results in loss of Cgv suppression, attenuated RSCv suppression, and enhanced PrL suppression, suggesting multiple pathways mediate DMN suppression. **(C)** E/I imbalance in PrL enhanced activity in the PrL but did not affect suppression in the RSC or Cg, consistent with the PrL's relative disengagement from the DMN and potential dual involvement to both the DMN and salience circuits. Results demonstrate how localized cellular disruption can lead to widespread network alterations robustly across levels of imbalance severity, by replicating findings from **Figure 4** in the presence of weaker E/I imbalance.